Structural characterization of the large soluble oligomers of the GTPase effector domain of dynamin

Jeetender Chugh[1], Amarnath Chatterjee[1], Ashutosh Kumar[1], Ram Kumar Mishra[2], Rohit Mittal[2] and Ramakrishna V. Hosur[1]

1 Department of Chemical Sciences and 2 Department of Biological Sciences, Tata Institute of Fundamental Research, Mumbai, India

Dynamin, a protein playing crucial roles in endocytosis, oligomerizes to form spirals around the necks of incipient vesicles and helps their scission from membranes. This oligomerization is known to be mediated by the GTPase effector domain (GED). Here we have characterized the structural features of recombinant GED using a variety of biophysical methods. Gel filtration and dynamic light scattering experiments indicate that in solution, the GED has an intrinsic tendency to oligomerize. It forms large soluble oligomers (molecular mass > 600 kDa). Interestingly, they exist in equilibrium with the monomer, the equilibrium being largely in favour of the oligomers. This equilibrium, observed for the first time for GED, may have regulatory implications for dynamin function. From the circular dichroism measurements the multimers are seen to have a high helical content. From multidimensional NMR analysis we have determined that about 30 residues in the monomeric units constituting the oligomers are flexible, and these include a 17 residue stretch near the N-terminal. This contains two short segments with helical propensities in an otherwise dynamic structure. Negatively charged SDS micelles cause dissociation of the oligomers into monomers, and interestingly, the helical characteristics of the oligomer are completely retained in the individual monomers. The segments along the chain that are likely to form helices have been predicted from five different algorithms, all of which identify two long stretches. Surface electrostatic potential calculation for these helices reveals that there is a distribution of neutral, positive and negative potentials, suggesting that both electrostatic and hydrophobic interactions could be playing important roles in the oligomer core formation. A single point mutation, I697A, in one of the helices inhibited oligomerization quite substantially, indicating firstly, a special role of this residue, and secondly, a decisive, though localized, contribution of hydrophobic interaction in the association process.

Dynamin is an important protein of the endocytic machinery in cells [1,2]. It has a modular structure characterized by the presence of an amino-terminal GTP-binding domain, a contiguous 'middle domain' of ill-defined function, a lipid binding pleckstrin homology domain followed by a coiled-coil 'assembly' domain and a proline-arginine rich domain at the extreme carboxy-terminal end. The GTPase domain is the most highly conserved domain within the members of the dynamin family. The functional roles of the various domains of dynamin have been described in great detail in several reviews [3]. It is thought that

Abbreviations

GED, GTPase effector domain; GST, glutathione-S-transferase; DLS, dynamic light scattering; TOCSY-HSQC, total correlated spectroscopy-heteronuclear single quantum coherence.

GTP-bound dynamin assembles in the form of rings around the necks of budding vesicles, and then a conformational change in the dynamin collar aids the scission of the vesicle from the parent membrane. The coiled-coil 'assembly' domain of the protein has been shown to mediate its assembly into oligomers [4] and has also been shown to possess an assembly stimulated GTPase accelerating property for the GTPase domain [5]. Therefore this domain is also termed the GTPase effector domain (GED). Further, the GED has been reported to be involved in multiple intramolecular and intermolecular interactions. It interacts with the amino-terminal GTP-binding domain of dynamin [6] and is also known to associate with other GED molecules, possibly mediating dynamin oligomerization [5]. In addition, the GED has also been shown to bind the middle domain of dynamin [7].

The above possibility of functional dissection of the dynamin protein into specific domains suggests that a detailed characterization of the intrinsic structural and dynamic characteristics of the individual domains has the potential to throw valuable light on the interactions of the individual domains, and the mechanism and variety of the overall functions of the full length protein. As of now, the structural characteristics of only the pleckstrin homology domain [8–10] and GTPase domain [11] have been reported in the literature. In this background we report here structural characterization of the GED using a variety of biophysical techniques. It turns out that the GED has a high tendency to form large multimers (molecular mass >600 kDa), in vitro. These oligomers exist in slow equilibrium with the monomers. The GED is seen to be largely helical in nature, and its oligomerization occurs via intermolecular packing of the helices. A single point mutation, I697A, significantly alters the association characteristics of the protein, implicating, first, a special role of the interactions at this site, and second, contribution of hydrophobic interactions in the association process.

Results and Discussion

The GED displays oligomer–monomer equilibrium in solution

We monitored the state of the isolated GED of dynamin under different conditions using gel filtration, dynamic light scattering and nuclear magnetic resonance. Gel filtration yields the molecular mass distribution in solution and when carried out on the isolated GED of dynamin at pH 5.7 using a Superdex 200 column showed that most of the protein appeared in the flow-through (Blue dextran, molecular mass 2000 kDa also appeared at the same place), and there was also a small peak seen corresponding to the monomer (Fig. 1A). This meant that the molecular mass of the major species was at least 600 kDa (the column
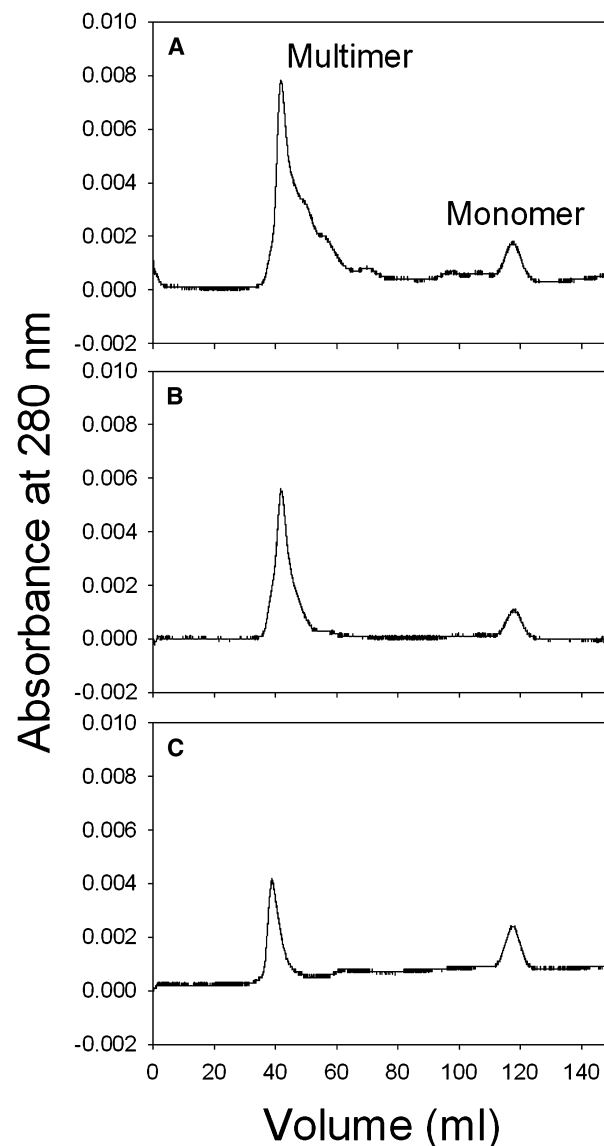
Fig. 1. Size exclusion chromatograms of: (A) Approximately 1.6 mg GED in 0.1 M phosphate buffer pH 5.7 at 27 °C, run on Hi Load 16/60 Superdex 200 column (Amersham), using a Bio-Rad BioLogic LP system, at a flow rate of 0.5 mL·min⁻¹; (B) Fractions corresponding to the oligomer peak from [38–48 mL in (A)] were concentrated and applied to same column; (C) Fractions corresponding to the monomer peak [114–124 mL in (A)] were concentrated and applied to the same column. In each case an oligomer peak is seen along with a peak corresponding to the GED monomer (15 kDa). The positions of molecular mass standards are indicated on top of (A).

cut-off is ≈ 600 kDa), although the possibility of oligomers of different sizes all above 600 kDa cannot be ruled out. In other words, the oligomers would consist of at least 40 monomer units; the molecular mass of the monomer is ≈ 15 kDa. When the flow-through was collected, concentrated and run through the column, there was again a small monomeric component, though the major portion was seen in the flow-through (Fig. 1B). The same observation was made when the monomeric fraction was collected, concentrated and run through the column (Fig. 1C). This indicated that the GED forms large soluble oligomers that are in equilibrium with the monomer and the energy barriers for the interconversion are not very high, as judged by easy interconversions. The population of the two would obviously depend upon the association constant. In the above experiments, the population of the monomer was estimated to be $\approx 17\%$ at a GED concentration of 100 µM, as calculated from areas under the respective peaks.

We next examined the oligomeric state of the GED using dynamic light scattering (DLS). DLS yields the hydrodynamic radius of a species in solution and thus reflects the state of association [12]. DLS measurements carried out at 27 °C, pH 5.7, at different concentrations ranging from 15 to 100 µM yielded uniformly a hydrodynamic radius of ≈ 22 nm for the major species of GED, as against a value of ≈ 2–3 nm typically expected for a monomeric protein of this size. This clearly indicated that the protein had associated into large oligomers even at micromolar concentrations (Fig. 2A). As a reference we show in Fig. 2B the DLS spectrum in the presence of 1% SDS, where the measured hydrodynamic radius for the major species is 3.37 nm, indicating loss of aggregation under these conditions. The same hydrodynamic radius was observed in 2.5% SDS as well. PAGE analysis at a SDS concentration of 2% showed a single band corresponding to the molecular mass of 15 kDa. Thus it is clear that the oligomer dissociates into monomers in the presence of 1% SDS in the solution. A simple calculation indicates that an oligomer sphere with a 22 nm radius would accommodate about 200 monomer spheres of 3 nm radii. Of course, this would be an extremely rough estimate because the hydration shells of the monomer and the oligomer would be different, the molecular shapes can deviate from spheres, the packing may not be closest, and the effective radius of the native monomer could be slightly smaller than that detected in SDS generated monomer. Nevertheless, the above estimate is fairly consistent with the lower bound of 40 monomers obtained from the gel filtration data.
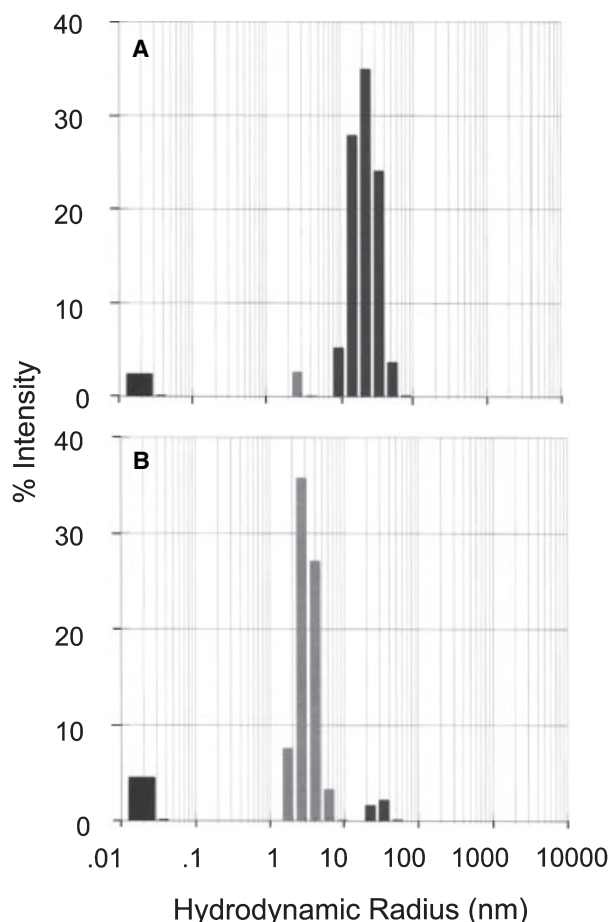

Fig. 2. Histogram of distribution of hydrodynamic radii obtained from 'regularization analysis' of data from dynamic light scattering experiments. (A) 100 µM GED in 0.1 M phosphate buffer, pH 5.7, 27 °C; average Rh = 22.37 nm; (B) 100 µM GED in 0.1 M phosphate buffer with 1% SDS (w/v), pH 5.7, 27 °C, average Rh = 3.37 nm.

Within the full length dynamin the GED interacts with the middle domain and the GTPase domain and thus the entire surface of the GED would not be exposed. This would limit the degree of association of dynamin which could provide a rationale that the building blocks of dynamin assembly are much smaller [1].

NMR characterization of the GED oligomers

The ^{1}H-^{15}N heteronuclear single quantum coherence (HSQC) spectrum of a protein displays one correlation peak for every amino acid residue (except prolines which do not have an amide proton) thereby providing detailed structural information at the single residue level. When a protein aggregates into a large mass, the correlation peaks buried in the interior of the
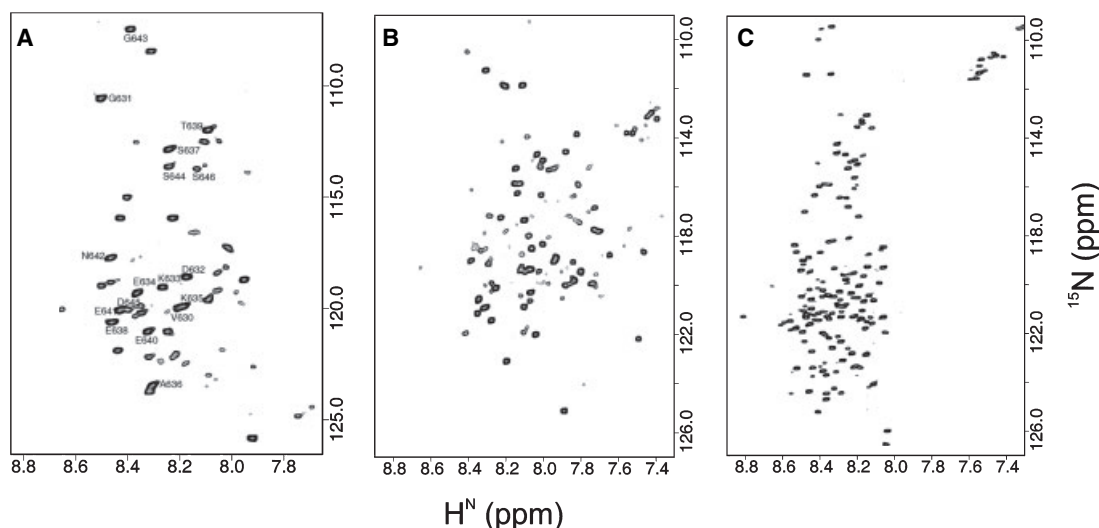
Fig. 3. (A) Fingerprint ^{1}H-^{15}N HSQC spectrum of GED in 0.1 M phosphate buffer at pH 5.7, 27 °C, showing 30 peaks (out of 136 residues) corresponding to the flexible portions of the oligomer. Assignments obtained for the stretch of 17 residues (V630–S646) have been marked. HSQC spectra of the protein under the same conditions as in (A) but in 2.5% SDS and 8 M urea are shown in (B) and (C), respectively.

aggregate become too broad to be observable. On the other hand, those residues which lie on the surface of the aggregate and are flexible still show correlation peaks. We thus carried out ^{1}H-^{15}N HSQC analysis on the isolated GED of dynamin (amino acids 618–753 of human dynamin I) expressed as a recombinant protein in bacteria. The ^{1}H-^{15}N HSQC spectrum of GED, under the same pH conditions as above, showed about 30 peaks (Fig. 3A), as opposed to the expected 132 peaks, indicating that approximately 30 residues were free and mobile while the rest were buried in the interior of the oligomers. These 30 peaks have line widths larger than one would normally see for a protein of this size indicating that these formed part of a large oligomer with an overall high rotational correlation time. As a reference we show in Fig. 3B the HSQC spectrum in 2.5% SDS which shows about 90 peaks, and in Fig. 3C the HSQC spectrum in 8 M urea, where more than 120 peaks are seen, indicating dissociation of the oligomer in to monomers; note, in all the three cases (Fig. 3A–C) the protein concentration was roughly the same. The HSQC spectra in SDS and urea have rather different peak dispersions indicating different degrees of denaturation in the two cases. In urea the protein is fully denatured as can be seen from the narrow chemical shift dispersion and uniformly sharp lines.

In order to gain further insight into which segment of the polypeptide chain is contributing to the association leading to the oligomers, we tried to obtain sequence specific assignment of the peaks seen in the HSQC spectra. These peaks, as mentioned before, represent flexible regions of the individual monomers in the oligomer and thus do not participate in the association process. Using a series of experiments such as HNN [13,14], HN(C)N [13,14], HNCA [15], HN(CO)CA [15], total correlated spectroscopy-heteronuclear single quantum coherence (TOCSY-HSQC) [16], 17 of the 30 peaks could be assigned to individual residues (see Supplementary material, Table 1). The assignments obtained are marked in Fig. 3A. Interestingly, these residues constitute a contiguous stretch at the amino terminal end of the GED.

The fact that sequential connectivities could be observed for 17 HSQC peaks in the triple resonance spectra indicates that all these peaks belong to the molecules in the same oligomer and the 17 residue flexible stretches of all the molecules in the oligomer, which are contributing to the signal, are chemically equivalent on the average. Otherwise one would have expected to see more than one set of such connectivities and obviously more peaks in the spectrum. For the remaining peaks sequential connectivities were observed only for a few short stretches, but this was not enough to locate these sequences specifically. It is quite likely that these belong to some short loops which may get formed during the assembling process.

In order to check whether the 17 residue segment had any secondary structural elements we calculated the secondary shifts (deviations of the observed chemical shifts from random values) for the C^α and H^α atoms. For α-helical structures, the secondary shifts of
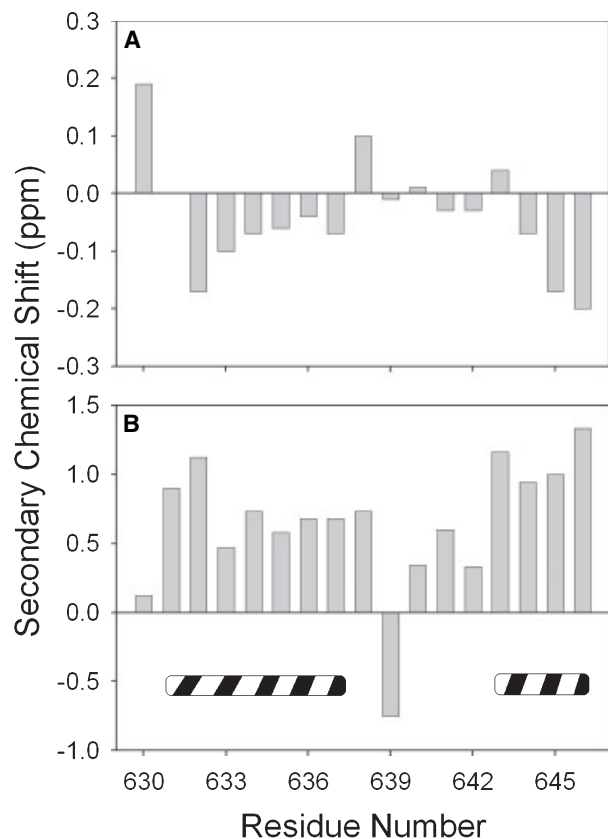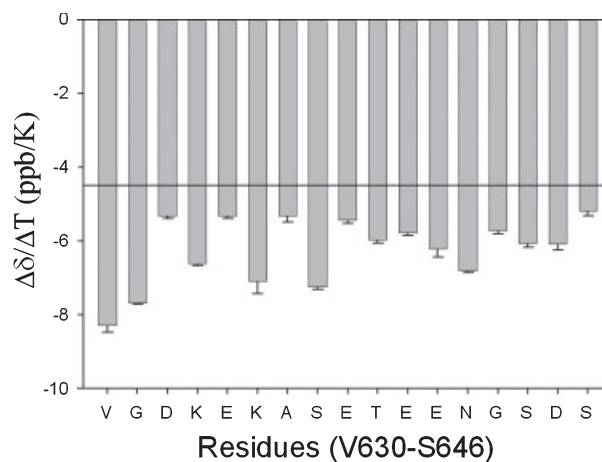
Fig. 4. Sequence corrected secondary chemical shifts. Deviations of observed chemical shifts from sequence corrected random coil values (A) H^{α}, (B) C^{α}, have been plotted against the residue number for the GED in 0.1 M phosphate buffer, pH 5.7 and 27 °C. Striped cylinders indicate α-helical propensities.

Fig. 5. Amide proton temperature coefficients for the 17 residues in the flexible region at the N-terminal. A horizontal line at −4.5 p.p.b.·K^{-1} is drawn to indicate the cut-off for identification of H-bonds.

C^{α} are positive, while those of H^{α} are negative. For β structures the trend is opposite [17,18]. The measured secondary shifts for the 17 residues in the present case are shown in Fig. 4. It is seen that the secondary shifts are small but not random. They indicate two stretches of perceptible helical conformations in this portion of the molecule in the oligomers. However, the NOE experiments did not show perceptible NH-NH NOEs, which must be expected for persistent helices. Similarly the magnitudes of the amide proton temperature co-efficients for all the 17 residues are larger than −4.5 p.p.b.·K^{-1} (Fig. 5) indicating absence of any intramolecular H bonds. Thus we conclude that the 17 residue stretch at the N-terminal has only some small propensity for formation of short helices, transiently, and the chain as such is highly dynamic.

Structure of the core of the oligomers

Because of the large size of the core of the oligomer, the NMR spectra do not show any signals from the interior of the core and thus do not give any information on its structural details. Nevertheless, we did derive useful insights into the structural aspects of the core of the oligomer from circular dichroism spectroscopy as described below.

Figure 6A shows the far UV circular dichroism spectrum of the GED at pH 5.7 and 27 °C. The spectrum shows distinct double well α-helix characteristics with minima at 208 and 222 nm. From this data, the helical content in the oligomer was estimated to be 45–50% (average of two calculations using the algorithms SELCON3 and CONTINLL ; see Supplementary material, Table S2, for details). Thus a large portion of the core of the oligomer is clearly helical in nature. Next, to gain a greater insight into the monomer association in the core, we tried to dissociate these oligomers into monomers using mild denaturing conditions so that the structural characteristics of the resulting monomeric units would be minimally disturbed. These monomers can then be probed further for the structural details. Among the different denaturants tried, SDS detergent appeared to satisfy our criteria to a large extent. As can be seen from DLS data in Fig. 2B, 1% SDS is sufficient to dissociate the oligomers into monomers. The HSQC spectrum of the protein in 2.5% SDS (Fig. 3B), which has good dispersion of peaks, indicates also that the protein retains a fair amount of structure; compare this with the fully denatured protein spectrum shown in Fig. 3C.

Far UV circular dichroism spectra of GED, recorded as a function of SDS concentration in the range 0–10% are shown in Fig. 6B. As shown below, these provide an extremely quantitative relation between the
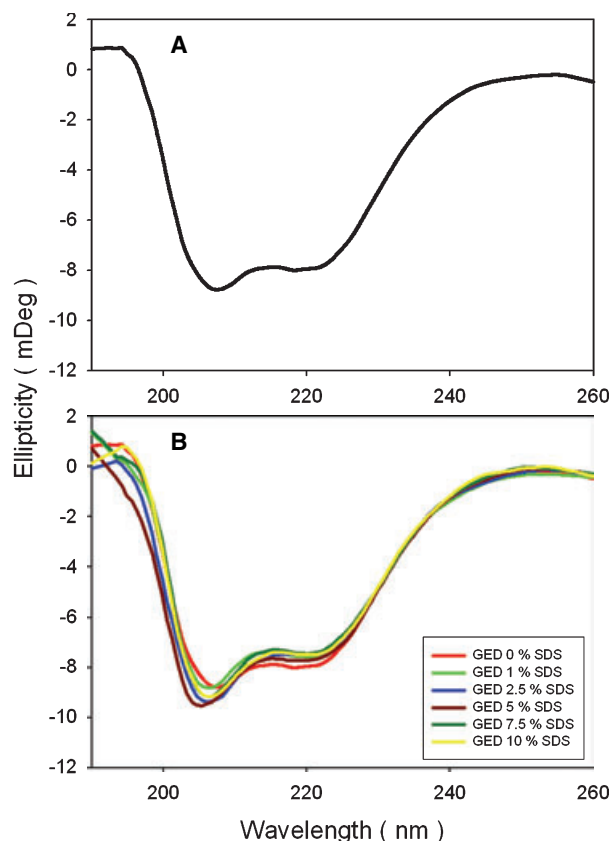
Fig. 6. Far UV circular dichroism spectra of (A) GED in 0.1 M phosphate buffer, pH 5.7 at 27 °C and (B) SDS titrations (0–10%) of GED at pH 5.7 at 27 °C in the wavelength range 190–260 nm. The data was smoothed using the negative exponential function in SIGMAPLOT. Protein concentration of 15 μM was used to study the secondary structure and an average of five spectral scans was taken.

structure of the core and the structural characteristics of the individual monomers. We observe in Fig. 6B that the spectra are nearly independent of the SDS concentration. Because 1% SDS is enough to break the oligomers into monomers (Fig. 2B), no change in the CD spectra on increasing the SDS percentage implies that SDS denaturation has already reached a saturation at 1% or that the SDS interaction does not disturb the helical characteristics of the chain in the present case. Secondly, the data also imply that the oligomers have helical characteristics identical to those of the SDS generated monomer. As there is no reason to think that SDS perturbation would be similar to the structural perturbations that may occur due to association, we conclude that the helical characteristics of the oligomer, represent, in fact, the intrinsic secondary structural preferences along the polypeptide chain.

Next, to determine the intrinsic secondary structural preferences and thus localize the individual helices in the monomers, sequence specifically, we used recent theoretical secondary structure prediction algorithms [19–22], which are derived from analysis of enormous structural data in the PDB database for sequence–structure correlations and have proved to be highly reliable. The results of such calculations by five different algorithms are shown in Fig. 7. It is satisfying to note that the predictions by the five algorithms are similar. Here, we like to point out also that the helical content that can be calculated from these predictions (≈ 50–55%) closely matches that estimated (45–50%) from the CD measurements. These establish the reliability of the predictions. Overall, we derive, as a consensus, two long helices (comprising amino acids 654–706 and amino acids 712–742 with probabilities, as per JUFO algorithm, of 80% and 83%, respectively). The C-terminal regions seem to be devoid of any definite structure. Because the flexible N-terminal is not contributing to the core, as seen from the NMR data, it follows that the core must be formed by packing of the two long helices from each of the monomer units. In an earlier study Okamoto *et al.* [4] showed that the peptides, amino acids 654–681 and amino acids 712–740, which are part of the above two helices had high helical characteristics and had tendencies to aggregate into tetramers and hexamers, respectively. The full length GED, however, oligomerizes into much larger mass as seen in the present work.

Hydrophobic association plays a crucial role in core formation

In order to probe the forces governing the association of the helices in the core of the oligomer, we calculated the electrostatic potential of the surfaces of the two long helical segments predicted from the above algorithms; these are shown in Fig. 8. The two opposite faces of the helices are shown in each case and we observe that in the longer helix, one of the surfaces is largely neutral. The opposite face has a distribution of neutral, positive (blue) and negative (red) potentials. The shorter helix has neutral surface at the two ends and a positive potential at the centre. These suggest that both hydrophobic association and electrostatic interactions of the helices could be playing roles in the core formation. Recently, Schmid *et al.* [23] showed that a single point mutation, I697K, can inhibit the assembly of dynamin. Location 697 lies in one of the helices in the GED, and the particular mutation changes a hydrophobic residue into a positively charged residue. This leads to an unfavorable energy factor for the packing. Therefore, the mutational perturbation of the association characteristics mentioned above provides strong and direct experimental evidence that
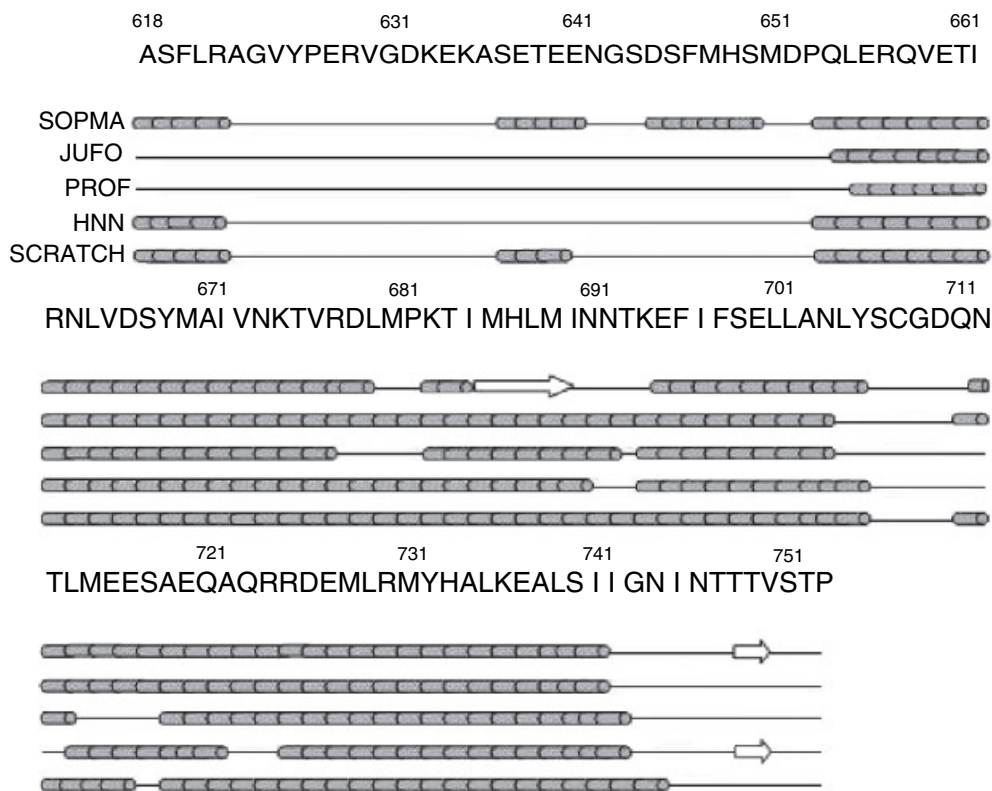
Fig. 7. Summary of the secondary structure prediction details of the GED using five different programs. Cylinders show α-helical regions, arrows show β-sheet and lines show random coils.

hydrophobic association of GED plays a crucial role in dynamin assembly. It also suggests that the interactions at the particular site, I697, have a very special role to play in the association. In order to gauge further the degree of this influence on the association we created a mutation, I697A, in the isolated GED being studied here, wherein a neutral residue is replaced by another neutral residue but with a smaller side chain. The results of gel filtration experiments carried out with this mutant GED under the same experimental conditions of protein concentration, pH and temperature, as with the wildtype protein, are shown in Fig. 9. Interestingly, this mutation is also seen to inhibit association of the protein quite significantly. At low concentration of 80 μM protein, there is essentially the monomer peak (Fig. 9A). This implies that the hydrophobic interactions of the I697 side chains in the native protein play a very dominant role in dictating the association characteristics of the protein. However, the mutation does not completely abolish association as can be seen from the data at higher protein concentrations in Fig. 9B. Nevertheless, the difference between the native protein and the mutant protein with regard to their association characteristics is clearly quite dramatic.

Conclusions

We have reported here the structural characteristics of the GED of dynamin probed using a variety of different biophysical techniques. Our experiments show that GED forms large oligomers (> 600 kDa) in solution, and also displays a rapid dynamic equilibrium between oligomers and monomers, with oligomers being the major species even at micromolar concentrations. This equilibrium, reported for the first time here, suggests a regulatory role for GED in dynamin assembly, via environmental perturbations which can shift these equilibria. From the NMR investigations on the oligomer, it is observed that about 30 residues are free and flexible and are not involved in the core formation. Out of these, a segment of 17 residues containing two short stretches of helical preferences has been identified to belong to the amino-terminal region of the GED. The CD data revealed that roughly 45–50% of the GED oligomer is helical. SDS-generated GED monomers exhibited similar helical content suggesting that oligomerization does not lead to changes in the secondary structure of the GED. Theoretical secondary structure prediction algorithms predicted two long stretches, amino acids 654–706 and amino acids 712–742,
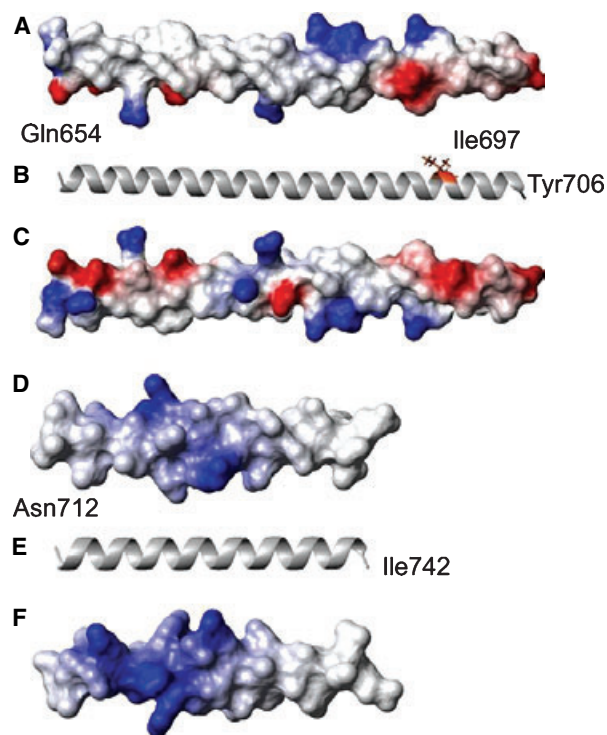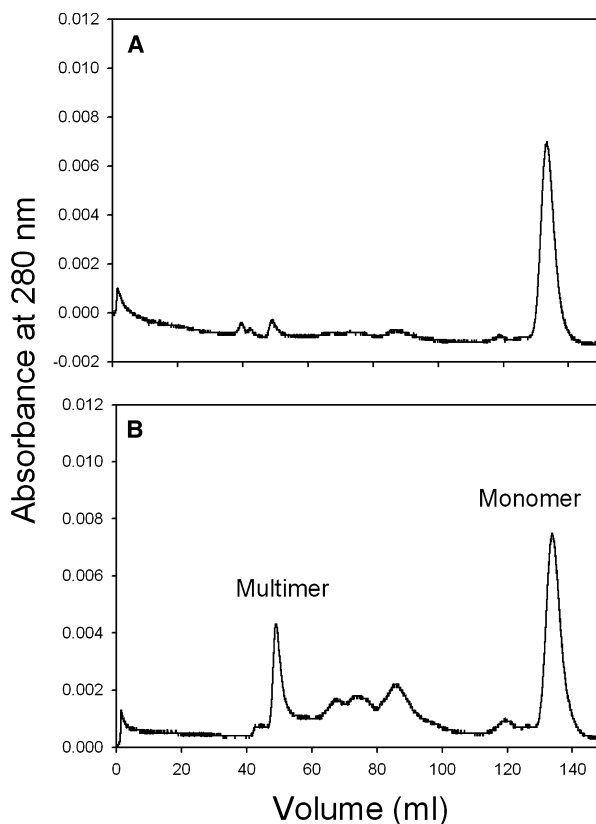
Fig. 8. Electrostatic potential calculations from MOLMOL (Wutrich *et al.*, Institute of Molecular Biology and Biophysics, Zurich, Switzerland) [25] for the two helical segments identified from the theoretical prediction algorithms. (A) and (C) show two opposite surfaces of the helix, amino acids 654–706, and (B) shows the helical structure. I697, the site of the mutation (see text) has been indicated. (D–F) show similar data for the helix, amino acids 712–742, as in the other helix in (A–C). In both cases red indicates negative potential, blue indicates positive potential and grey indicates neutral surface.

Fig. 9. Size exclusion chromatograms as in Fig. 1 for the I697A mutant of GED at two different protein concentrations, 80 μM (A) and 400 μM (B). All the other experimental conditions are the same as in Fig. 1.

to be helical in nature, implicating that these could be the main contributors to the core of the oligomer. I697 located in one of the above helices appears to have a special role in the association process, as mutation of this Ile to Ala inhibited GED association quite significantly. This also indicates a significant contribution of hydrophobic interactions in the packing of the helices in the core of the oligomer. Because GED is the primary driver of dynamin assembly, all these observations would throw valuable light on the extent and mechanism of the assembly of dynamin, depending upon the experimental conditions and sequence variations.

Experimental procedures

Protein expression and purification

cDNA corresponding to the GTPase effector domain (amino acids 618–753) of human dynamin I protein was subcloned into the bacterial expression plasmid pGEX4T1 (Amersham Biosciences Corp, Piscataway, NJ, USA) cut with *Eco*RI and *Sal*I. The clone was confirmed by multiple restriction digests and DNA sequencing and then transformed into *Escherichia coli* BL21 cells. Expression of the glutathione-*S*-transferase (GST)-fusion protein was induced with 100 μM of isopropyl-β-D-thiogalactopyranoside for 8 h at 28 °C. The harvested culture was lysed in TEND buffer (20 mM Tris, pH 7.4, 1 mM EDTA, 150 mM NaCl, and 1 mM dithiothreitol) containing lysozyme and protease inhibitors. The lysed cells were sonicated and spun at 100 000 ***g*** for 45 min to obtain a clear supernatant. The supernatant was incubated with glutathione-Sepharose beads (Amersham) for 2 h at 4 °C to allow binding of overexpressed GST-GED recombinant protein. The beads were then washed with TEND buffer. Protein coated beads were incubated with thrombin (Sigma-Aldrich, St. Louis, MO, USA) for 20 h at 25 °C to remove the GST tag. GST clipping was observed by running samples on 16% SDS/PAGE. The supernatant containing primarily the free GED was then passed over GSH-sepharose column repeatedly to remove any contaminating GST or GST-GED. The

pure GED protein thus obtained was dialysed against 0.1 M phosphate buffer (pH 5.7) containing 1 mM dithiothreitol, 1 mM EDTA and 150 mM NaCl.

Site directed mutagenesis

Point mutations were performed on the gene for GED from human Dynamin I in pGEX4T1 vector by the QuickChange method (Stratagene, La Jolla, CA) using the oligonucleotides I697A-f 5′-GATTAATAATACCAAGGAGTTCGCCTTC TCGG-3′ and I697A-r 5′-CCGAGAAGGCGAACTCC TTGGTATTATTAATC-3′ (Sigma Aldrich). The construct was confirmed by sequencing (Bangalore-Genei, Peenya, Bangalore, India).

Gel filtration studies

Size exclusion chromatography was performed using a Hi Load 16/60 Superdex 200 column (Amersham, cut-off, ≈ 600 kDa) with buffer (0.1 M phosphate, pH 5.7, 1 mM EDTA, 1 mM dithiothreitol, 150 mM NaCl) at a flow rate of 1.0 mL·min^{-1} with absorbance monitored at 280 nm using Bio-Rad (Hercules, CA, USA) BioLogic LP system. Gel filtration protein standards (Amersham) were used to calibrate the column. Recombinant GED (100 μM, 1 mL) was centrifuged at 15 600 *g* at 4 °C for 10 min and the supernatant was applied to the Hi Load 16/60 Superdex 200 column. Fractions corresponding to 38–48 mL (Fig. 1A) were collected and concentrated in an ultra-filtration cell (Amicon, Millipore, Billerica, MA, USA) with 3 kDa cut-off membrane (Millipore) under nitrogen atmosphere and the volume was reduced to 1 mL, and reapplied to the Hi Load 16/60 Superdex 200 column (Fig. 1B). Fractions corresponding to 114–124 mL (Fig. 1A) were processed in a similar manner (Fig. 1C).

Dynamic light scattering measurements

DLS experiments were performed on a DynaPro-MS800 instrument (Protein Solutions Inc., Charlottesville, VA, USA) that monitors the scattered light at 90°. At least 20 measurements each of 10 s duration were collected. Buffer solutions were filtered through 20 nm filters (Whatman Anodisc 13, catalog no. 6809–7003, Whatman plc, Brentford, UK). Extreme care was taken to reduce the contamination of samples by dust. 'Regularization' software provided by the manufacturer was used in analyzing the results for obtaining distribution of hydrodynamic radius of particles in the solution. Standard synthetic beads of 6 nm diameter (provided by the manufacturers) and BSA (typical hydrodynamic radius 3.0 nm) were used as standards. GED concentrations used varied from 15 to 100 μM, in a 50 μL volume cuvette, in phosphate buffer with and without 1% (w/v) SDS. All measurements were done at 27 °C.

NMR spectroscopy

For NMR studies, isotopically labeled protein was prepared from *E. coli* BL21 cells harboring the GST-GED expression clone grown in M9 minimal medium containing ^{15}NH$_4$Cl and ^{13}C-glucose. The protein purified as described above was concentrated to 1 mM and exchanged with buffer (0.1 M phosphate, pH 5.7, 1 mM EDTA, 1 mM dithiothreitol, 150 mM NaCl) in an ultra-filtration cell (Amicon) using 3 kDa cut-off membrane (Millipore). The final volume of the sample was ≈ 550 μL containing 10% (v/v) D$_2$O.

All NMR experiments were performed at 27 °C on a Varian (Palo Alto, CA, USA) Unity-plus 600 MHz NMR spectrometer equipped with pulse-shaping and pulse field gradient capabilities. For the HNCA [15] spectrum the delay T$_N$ was 12.5 ms, and 32 and 80 complex points were used along t$_1$ and t$_2$ dimensions, respectively. The HN(CO)CA [15] spectrum was recorded with the same T$_N$ parameters, and same number of t$_1$ and t$_2$ points. TOCSY-HSQC and NOESY-HSQC [16] were recorded with a mixing time of 80 ms and 150 ms, respectively, 32 complex points along ^{15}N (t$_1$) dimension and 80 complex points along ^{1}H (t$_2$) dimension. HNN and HN(C)N [13,14] were recorded with 32 complex t$_1$ points (^{15}N) and 32 complex t$_2$ points (^{15}N). HSQC were recorded with 256 t$_1$ increments. Amide proton temperature coefficients were measured by recording HSQC spectra in the temperature range, 21–39 °C, at 3 °C intervals.

Circular dichroism measurements

The far-UV CD data were recorded on a Jasco (Easton, MD, USA) J600 spectro-polarimeter in the 190–260 nm region using a rectangular cuvette of 1 mm path length thermostated at 27 °C. A protein concentration of 15 μM was used in these measurements. All CD spectra measured were baseline corrected by the buffer. The secondary structure elements of GED were computed from the data using a computer program developed by Johnson and colleagues for this purpose [24]. Spectral deconvolution was performed on the average of five spectral scans. The data was smoothed using the negative exponential function in SIGMA-PLOT (Systat Software, Point Richmond, CA, USA) for plotting; however, it was not smoothed for deconvolution. Protein solutions of 15 μM were equilibrated with various SDS concentrations, ranging from 0 to 10% (w/v), for 12 h at 27 °C before the spectra were recorded.

References

1 Praefcke GJ & McMahon HT (2004) The dynamin superfamily: universal membrane tubulation and fission molecules? *Nat Rev Mol Cell Biol* **5**, 133–147.

2 Conner SD & Schmid SL (2003) Regulated portals of entry into the cell. *Nature* **422**, 37–44.

3 Hinshaw JE (2000) Dynamin and its role in membrane fission. *Annu Rev Cell Dev Biol* **16**, 483–519.

4 Okamoto PM, Tripet B, Litowski J, Hodges RS & Vallee RB (1999) Multiple distinct coiled-coils are involved in dynamin self-assembly. *J Biol Chem* **274**, 10277–10286.

5 Sever S, Muhlberg AB & Schmid SL (1999) Impairment of dynamin's GAP domain stimulates receptor-mediated endocytosis. *Nature* **398**, 481–486.

6 Muhlberg AB, Warnock DE & Schmid SL (1997) Domain structure and intramolecular regulation of dynamin GTPase. *EMBO J* **16**, 6676–6683.

7 Smirnova E, Shurland DL, Newman-Smith ED, Pishvaee B & van der Bliek AM (1999) A model for dynamin self-assembly based on binding between three different protein domains. *J Biol Chem* **274**, 14942–14947.

8 Timm D, Salim K, Gout I, Guruprasad L, Waterfield M & Blundell T (1994) Crystal structure of the pleckstrin homology domain from dynamin. *Nat Struct Biol* **1**, 782–788.

9 Downing AK, Driscoll PC, Gout I, Salim K, Zvelebil MJ & Waterfield MD (1994) Three-dimensional solution structure of the pleckstrin homology domain from dynamin. *Curr Biol* **4**, 884–891.

10 Fushman D, Cahill S, Lemmon MA, Schlessinger J & Cowburn D (1995) Solution structure of pleckstrin homology domain of dynamin by heteronuclear NMR spectroscopy. *Proc Natl Acad Sci USA* **92**, 816–820.

11 Reubold TF, Eschenburg S, Becker A, Leonard M, Schmid SL, Vallee RB, Kull FJ & Manstein DJ (2005) Crystal structure of the GTPase domain of rat dynamin. *Proc Natl Acad Sci USA* **102**, 13093–13098.

12 Schmitz KS (1990) *An Introduction to Dynamic Light Scattering by Macromolecules*. Academic Press, San Diego, California.

13 Panchal SC, Bhavesh NS & Hosur RV (2001) Improved 3D triple resonance experiments, HNN and HN(C)N, for H^N and ^{15}N sequential correlations in ($^{13}C, ^{15}N$) labeled proteins: application to unfolded proteins. *J Biomol NMR* **20**, 135–147.

14 Bhavesh NS, Panchal SC & Hosur RV (2001) An efficient high-throughput resonance assignment procedure for structural genomics and protein folding research by NMR. *Biochemistry* **40**, 14727–14735.

15 Ferentz AE & Wagner G (2000) NMR spectroscopy: a multifaceted approach to macromolecular structure. *Q Rev Biophys* **33**, 29–65.

16 Fesik SW & Zuiderweg ER (1990) Heteronuclear three-dimensional NMR spectroscopy of isotopically labelled biological macromolecules. *Q Rev Biophys* **23**, 97–131.

17 Wishart DS & Sykes BD (1994) The ^{13}C chemical-shift index: a simple method for the identification of protein secondary structure using ^{13}C chemical-shift data. *J Biomol NMR* **4**, 171–180.

18 Wishart DS, Bigam CG, Holm A, Hodges RS & Sykes BD (1995) ^1H, ^{13}C and ^{15}N random coil NMR chemical shifts of the common amino acids. I. Investigations of nearest-neighbor effects. *J Biomol NMR* **5**, 67–81.

19 Baldi P, Brunak S, Frasconi P, Soda G & Pollastri G (1999) Exploiting the past and the future in protein secondary structure prediction. *Bioinformatics* **15**, 937–946.

20 Combet C, Blanchet C, Geourjon C & Deleage G (2000) NPS@: network protein sequence analysis. *Trends Biochem Sci* **25**, 147–150.

21 Meiler J, Mueller M, Zeidler A & Schmaeschke F (2001) Generation and evaluation of dimension-reduced amino acid parameter representations by artificial neural networks. *J Mol Modeling* **7**, 360–369.

22 Pollastri G, Przybylski D, Rost B & Baldi P (2002) Improving the prediction of protein secondary structure in three and eight classes using recurrent neural networks and profiles. *Proteins* **47**, 228–235.

23 Song BD, Yarar D & Schmid SL (2004) An assembly-incompetent mutant establishes a requirement for dynamin self-assembly in clathrin-mediated endocytosis *in vivo*. *Mol Biol Cell* **15**, 2243–2252.

24 Johnson WC (1999) Analyzing protein circular dichroism spectra for accurate secondary structures. *Proteins* **35**, 307–312.

25 Koradi R, Billeter M & Wuthrich K (1996) MOLMOL: a program for display and analysis of macromolecular structures. *J Mol Graph* **14**, 51–32.

Supplementary material

The following supplementary material is available online:

Table S1. Chemical shifts of the assigned stretch of 17 residues in the GED at pH 5.7, 27 °C

Table S2. Secondary structure calculation details from Circular Dichroism spectra of GED at pH 5.7, 27 °C using SELCON3 and CONTINLL under four different basis sets*.

This material is available as part of the online article from http://www.blackwell-synergy.com